Nonplanar, Subsonic, Three-Dimensional Oscillatory Piecewise Continuous Kernel Function Method

I. Lottati* and E. Nissim†
Technion—Israel Institute of Technology, Haifa, Israel

The rapid convergence characteristics and high accuracy of the three-dimensional piecewise continuous kernel function method are tested on a nonplanar configuration. The nature of the singularity of the three-dimensional kernel function for the nonplanar configuration is examined and anomalies associated with almost adjoining lifting surfaces are explained. Applications are made using the standard AGARD wing-tail configuration and the interference aerodynamic forces are compared with results obtained using other numerical methods.

Introduction

THE general problem of interference between nonplanar surfaces was discussed by Landahl and Stark,[1] Laschka,[2] Ashley and Rodden,[3] and others. These reviews contained surveys on linearized theoretical methods for analyzing nonplanar lifting-surface interference problems in subsonic, steady, and unsteady flows. An extensive survey on numerical methods used to compute aerodynamic forces on interfering lifting surfaces was conducted by Rodden[4] under the sponsorship of the Structures and Materials Panel of AGARD. The survey compares a number of numerical methods used to compute aerodynamic forces on interfering surfaces throughout the Western World. The different methods are tested using examples chosen by AGARD in order to permit an evaluation of the various methods.

In the present work, the extension of the piecewise continuous kernel function method (PCKFM)[5-7] to compute aerodynamic forces on a nonplanar configuration is described. The nature of the singularity of the nonplanar kernel function is examined and its characteristics are taken into consideration while developing the nonplanar version of the PCKFM. The numerical results obtained using the PCKFM for the above-mentioned AGARD examples are compared with results obtained using other methods.

Description of the Nonplanar PCKFM

In general, PCKFM[5-7] can cope successfully with unknown pressure singularities provided their location is known. Therefore, the wing surface is divided into boxes such that pressure singularities are permitted to be along the boundaries of the boxes. Unlike the doublet-lattice method,[8] the boxes used by the PCKFM can be as large as possible provided they exclude pressure discontinuities (implying also discontinuities in the derivatives of the pressure) from lying within the regions defined by the boundaries of the boxes. The pressure distribution in each box is then represented by a set of continuous polynomials spanning the regions between the adjoining singularities. In order to accelerate convergence, pressure singularities are assumed to be known only along the boundaries of the wing, or, more specifically, the forms of the leading-edge (LE), trailing-edge (TE), and wingtip pressure singularities are assumed to be known and are treated in the analysis as such. All other pressure singularities are ignored during the analysis, and their consideration is limited to the determination of the boundaries between the different boxes. The problems associated with the basic three-dimensional PCKFM were treated in Refs. 5-7. Additional problems which arise from the three-dimensional nonplanar flow configurations and which require the formulation of numerical techniques for the successful application of the method are addressed in this paper.

An example of a wing with geometrical discontinuities divided into boxes is given in Fig. 1. The pressure distribution in each of the boxes formed by the PCKFM can, therefore, be represented in general terms by the following expression:

$$\frac{\Delta p(\xi,\eta)}{q}=\sum_{J=1}^{\mathrm{ns}}\sum_{i=1}^{\mathrm{nc}}A_m W(\eta)P_j(\eta)w(\xi)p_i(\xi)/c(\eta) \qquad (1)$$

where $\Delta p(\xi,\eta)$ represents the distribution of the pressure difference across the box, $q=\rho v^2/2$ is the dynamic pressure, A_m a scalar coefficient, nc and ns the number of chordwise and spanwise pressure polynomials, respectively, and $m=(j-1)^*\mathrm{nc}+i$. The parameters ξ and η represent the coordinates in the chordwise and spanwise directions, respectively. $w(\xi)$ and $W(\eta)$ represent the assumed singularities in the chordwise and spanwise directions, respectively. Each polynomial $p_i(\xi)$ and $P_j(\eta)/c(\eta)$ is orthogonal to its respective weight function $w(\xi)$ and $W(\eta)$.

The relationship between the pressure distribution over the wing and its resulting downwash is given by

$$\frac{w(w,y,z)}{v}=\frac{1}{8\pi}\int\int_S\frac{\Delta p(\xi,\eta)}{q}\frac{K_p(x-\xi,y-\eta,z-\zeta,k,M)}{r^2}\mathrm{d}\xi\mathrm{d}\eta \qquad (2)$$

where

$\dfrac{w(x,y,z)}{v}$ = vertical nondimensional velocity [downwash at any collocation point (x,y,z) of the wing]

$K_p(\ )$ = modified kernel function (without the second-order pole) that relates the downwash at the collaction point (x,y,z) caused by a unit pressure difference at point (ξ,η,ζ)

k = reduced frequency, $=\omega b/v$ (ω is the frequency of oscillation and b a reference length)

M = Mach number

S = area of the wing configuration

Received Oct. 6, 1984; revision received July 29, 1985.

*Senior Lecturer, Department of Aeronautical Engineering
†Professor, Department of Aeronautical Engineering. Member AIAA.

r^2 = a second-order pole for the coplanar and almost planar interference configurations, $(y-\eta)^2+(z-\zeta)^2$

x,y,z = coordinates of the collocation point

ξ,η,ζ = coordinates of the doublet point

The integral in Eq. (2) is evaluated by dividing the wing into four regions[5] and performing the numerical integration separately, taking into account the strong singularity of the second-order pole [r^{-2} in Eq. (2)].

Laschka,[9] Rodemich (Vivian and Andrew[10]), and Landahl[11] have given the subsonic acceleration potential kernel function for nonplanar lifting surfaces as

$$K(x_0,y_0,z_0,k,M)=\exp(-i\omega x_0/v)\,(K_1T_1+K_2T_2)r^{-2} \tag{3}$$

where x_0 is the distance between the sending and receiving points parallel to the freestream ($x_0=x-\xi$), and

$$T_1=\cos(\gamma_r-\gamma_s) \tag{4}$$

where γ_r and γ_s are the dihedral angles of the receiving and sending points, respectively, and

$$T_2=(z_0\cos\gamma_r-y_0\sin\gamma_s)\,(z_0\cos\gamma_s-y_0\sin\gamma_s)r^{-2} \tag{5}$$

where y_0 is the distance between the sending and receiving points perpendicular to the freestream in the span direction ($y_0=y-\eta$), and z_0 is the difference in height between the sending and receiving points ($z_0=z-\zeta$). K_1 and K_2 are regular functions defined in Ref. 4.

Rodden et al.[12] reported some unusual anomalies using the kernel function as given by Eq. (3) and suggested that Eq. (3) must be written as

$$k(x_0,y_0,z_0,k,M)=\exp(-i\omega x_0/v)\,(K_1T_1r^{-2}+K_2T_2^*r^{-4}) \tag{6}$$

The form of Eq. (6) is suggested in order to eliminate the large errors encountered in the computation of aerodynamic forces when the interference lifting surfaces are only a small distance apart in height $z_0/s \ll 1$, where s represents the wing semispan.

Equation (6) effectively replaces T_2 by $T_2^*r^{-2}$ with T_2^* being a regular function. This implies that T_2 is necessarily singular, which is clearly untrue since T_2 can be brought to the form

$$T_2=\left(\frac{z_0}{r}\cos\gamma_r-\frac{y_0}{r}\sin\gamma_s\right)\left(\frac{z_0}{r}\cos\gamma_s-\frac{y_0}{r}\sin\gamma_s\right) \tag{7}$$

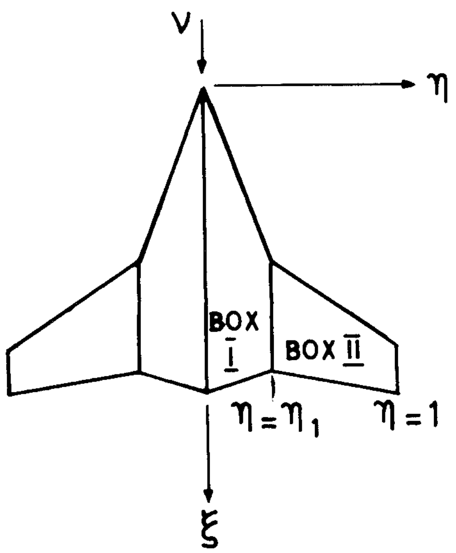

Fig. 1 Example of wing with geometrical discontinuities (breakpoints in both leading and trailing edges).

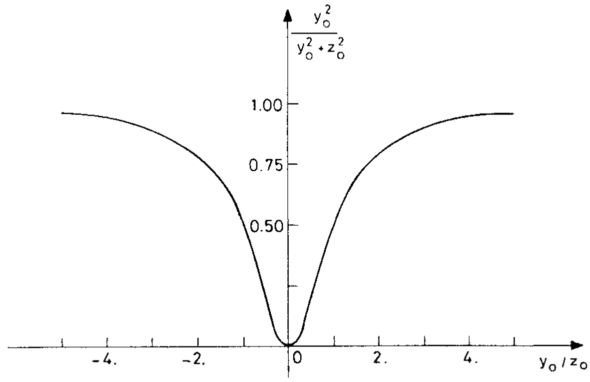

Fig. 2 Plot of y_0^2/r^2 vs y_0/z_0.

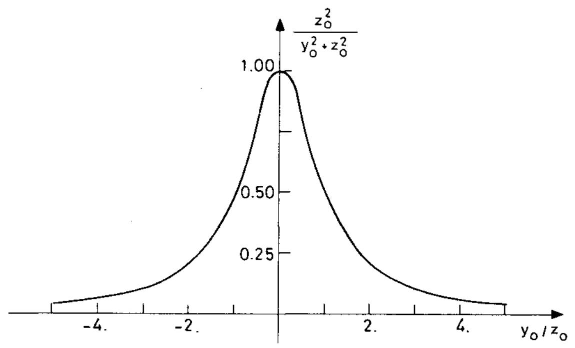

Fig. 3 Plot of z_0^2/r^2 vs y_0/z_0.

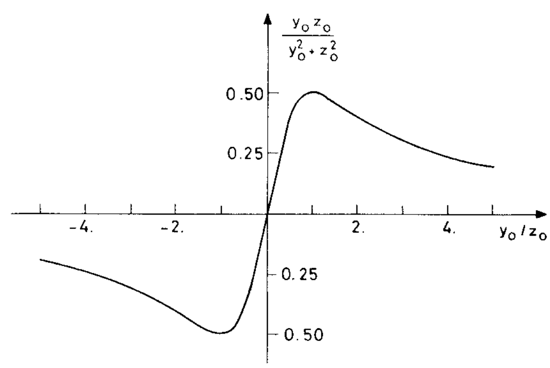

Fig. 4 Plot of y_0z_0/r^2 vs y_0/z_0.

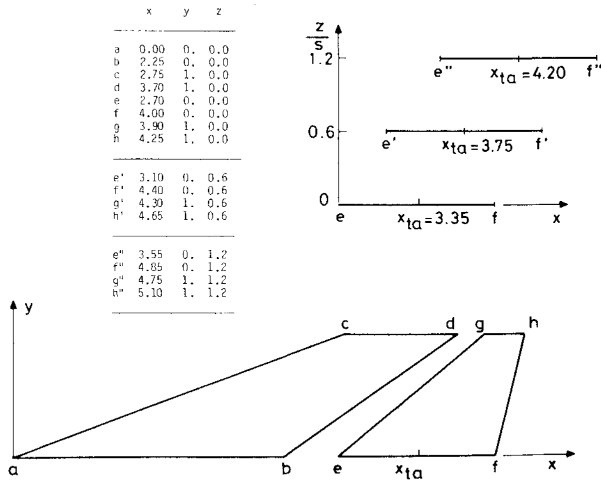

	x	y	z
a	0.00	0.	0.0
b	2.25	0.	0.0
c	2.75	1.	0.0
d	3.70	1.	0.0
e	2.70	0.	0.0
f	4.00	0.	0.0
g	3.90	1.	0.0
h	4.25	1.	0.0
e'	3.10	0.	0.6
f'	4.40	0.	0.6
g'	4.30	1.	0.6
h'	4.65	1.	0.6
e"	3.55	0.	1.2
f"	4.85	0.	1.2
g"	4.75	1.	1.2
h"	5.10	1.	1.2

Fig. 5 AGARD wing-horizontal tail, nonplanar configuration.

Table 1 Convergence study of AGARD wing-tail (coplanar), steady lift curve slope ($k=0$)

PCKFM			Doublet-lattice method		
No. of pressure polynomials			No. of boxes		
Chordwise	Spanwise	$C_{L\alpha}$	Chordwise	Spanwise	$C_{L\alpha}$
3	3	1.9036	9	12	1.9766
4	4	1.9036	11	12	1.9781
5	5	1.9021	14	12	1.9793
			18	12	1.9795
			22	12	1.9794

Table 2 Convergence study of AGARD wing-tail (coplanar) in oscillating plunging mode ($k=1.5$)

PCKFM			Doublet-lattice method		
No. of pressure polynomials			No. of boxes		
Chordwise	Spanwise	$C_L/ik(h/s)$	Chordwise	Spanwise	$C_L/ik(h/s)$
3	3	$4.409+i2.881$	9	12	$3.831+i2.916$
4	4	$4.401+i2.856$	11	12	$3.961+i2.964$
5	5	$4.415+i2.861$	14	12	$4.159+i2.973$
			18	12	$4.297+i2.958$
			22	12	$4.357+i2.954$

rewritten as

$$T_2=\sin(\varphi-\gamma_r)\sin(\varphi-\gamma_s) \tag{8}$$

where

$$z_0/r=\sin\varphi \quad \text{and} \quad y_0/r=\cos\varphi \tag{9}$$

Equation (8) shows that T_2 cannot possibly be singular and, therefore, the representation of Rodden et al.[12] which attributes a double-pole singularity to T_2, is clearly artificial.

Nevertheless, while running the PCKFM to compute the aerodynamic forces on an AGARD configuration[4] with two adjoining lifting surfaces (in the vertical direction), anomalies similar to those reported by Rodden et al.[12] were encountered when $z_0/s \ll 1$. The anomalies encountered when $z_0/s \ll 1$ will be investigated in the following:

Let T_2 be expanded to assume the form

$$T_2=\frac{z_0^2}{r^2}\cos\gamma_r\cos\gamma_s+\frac{y_0^2}{r^2}\sin\gamma_r\sin\gamma_s-\frac{z_0y_0}{r^2}\sin(\gamma_r+\gamma_s) \tag{10}$$

The expressions z_0^2/r^2, y_0^2/r^2, and z_0y_0/r^2 appearing in Eq. (10) are plotted vs y_0/z_0 in Figs. 2-4. The rapid changes in these expressions can be seen in those figures when y_0/z_0 lies in the range $-3<y_0/z_0<3$. At this stage, it should be remembered that the range of the spanwise integration of Eq. (2) varies from $-s$ *to* $+s$, therefore, whenever $z_0/s \ll 1$, the parameter y_0/z_0 $[=(y_0s)/(z_0/s)]$ changes from a large negative number to a large positive number and thus crossing the above region of very rapid variations ($|y_0/z_0|<3$). Applying the Gauss quadrature techniques for the spanwise integration of Eq. (2), one cannot take into account this rapid variation of T_2 (whenever $z_0/s \ll 1$) unless a very large number of integration points are taken to perform the integral. This rapid change in T_2 might be the source of the anomalies encountered for small differences in height of the interfering surfaces as reported in Ref. 4. It appears that the artificial insertion of a double-pole singularity in T_2 (which does not exist in reality), as suggested by Rodden et al.[12] can diminish the rapid variation of T_2^* vs y_0/z_0 for small values of z_0/s.

Another way to cope with the rapid variation of T_2 is to divide the spanwise integration of Eq. (2) to take into account the rapid variation of T_2 with respect to y_0/z_0. In other words, one can divide the spanwise region of integration into subregions to cope with the rapid variation of T_2. The Gauss integration technique, with only a small number of points in each of these subregions (two to three points of integration in each region), can then be readily employed. The recommended subregions of integration, as implemented in the PCKFM computer code, are $0<|y_0/z_0|<0.7$, $0.7<|y_0/z_0|<2$, and $|y_0/z_0|>2$. Recomputation of the aerodynamic forces on the aforementioned AGARD interference configuration, using the described spanwise-piecewise integration procedure, cured the anomalies encountered earlier. As a result, the modified PCKFM nonplanar version produced a smooth variation of the aerodynamic forces vs the difference in height between the two interfering surfaces (for small z_0/s). At this stage one should mention that the implementation of the above results in a doublet-lattice computer code is by no means simple, since it implies that the span of the boxes be a function of y_0/z_0. This yields an unrealistically large number of spanwise boxes whenever z_0/y_0 can become small, and it explains why the solution given by Rodden et al.[12] is preferable for the doublet-lattice method.

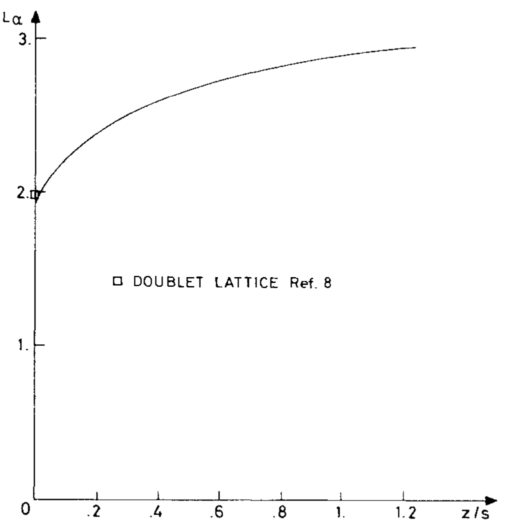

Fig. 6 Variation of the lift coefficient $C_{L\alpha}$ of the nonplanar AGARD configuration in steady flow vs the tail height, computed by the PCKFM.

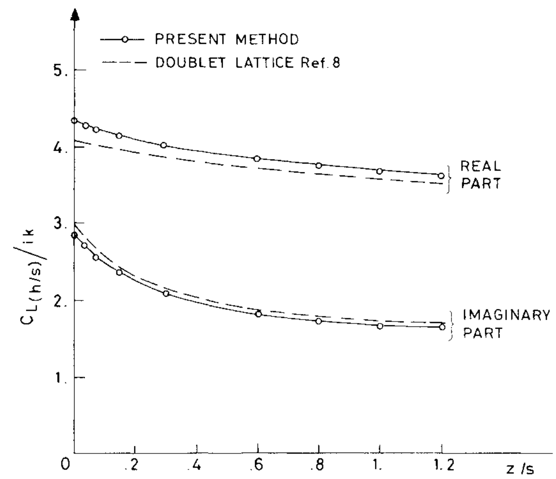

Fig. 7 Comparison study of the variation of the lift coefficient for the AGARD wing-tail configuration oscillated in a heave mode ($k=1.5$) vs the tail height, computed by the PCKFM and the doublet-lattice method.[8]

Results

The first example tested is the AGARD configuration shown in Fig. 5 and referred to in Ref. 8. The horizontal tail of the configuration is placed at different heights and distances from the wing, as shown in Fig. 5. The smooth variation of the lift coefficient (C_{L_α}) vs the variation in height of the horizontal tail (above the plane of the wing) is represented in Fig. 6. Note that C_{L_α} is normalized to the area of the wing only. The results for the coplanar case, as computed by the method of Ref. 8, are also shown in Fig. 6 for comparison.

The unsteady aerodynamic coefficients for this same configuration undergoing a heave mode of oscillation are shown in Fig. 7. The aerodynamic coefficients for a single reduced frequency are computed for various positions of the horizontal tail and for different values of z_0/s. The results computed by the PCKFM are compared with those obtained from the doublet-lattice method.[8] In Fig. 7, the aerodynamic coefficients are normalized to the semispan of the configuration. The results of the present method compared very well with those computed by the doublet-lattice method of Ref. 8.

Note that the preceding results using the PCKFM were obtained by representing the AGARD configuration by two boxes (the wing and the tail, one box each). Three chordwise and three spanwise pressure polynomials (per box) were used. As already stated earlier, the chordwise polynomials are orthogonal to the LE and TE singularities, while the spanwise pressure polynomials are orthogonal to the wingtip singularity (this applies for both the wing and tail surfaces). While computing the aerodynamic coefficients for the AGARD configuration, the PCKFM thus required the determination of 18 unknown pressure coefficients (A_m). Even though this number of assumed pressure polynomials is relatively small, the results compare very well with those obtained using the doublet-lattice method in Ref. 8 (using 264 boxes, that is 264 unknowns).

Convergence studies are conducted at this point in order to verify that the differences between the values of the aerodynamic coefficients, as obtained by the present method and those obtained by the doublet-lattice method,[8] do not originate from the low-order polynomials assumed in the present paper. Table 1 presents a convergence study of the lift coefficient $C_{L\alpha}$ of the AGARD coplanar wing-tail configuration in steady flow, and it shows that, in all cases, the value of $C_{L\alpha}$ is essentially converged for both the PCKFM and the doublet-latice method. Table 2 presents a similar convergence study relating to the same wing while performing a plunging oscillation at a reduced frequency $k=1.5$. Here it can be seen that the PCKFM shows convergence in all cases, while the doublet-lattice values vary continuously with the number of boxes on the wing.

Additional applications are made using the wing/horizontal tail configuration shown in Fig. 5, assuming various antisymmetric vibration modes of the wing and tail. Four antisymmetric vibration modes are assumed; two modes for the wing and two modes for the tail. The wing modes are: wing twisting represented by $f_{1w}=(y/s)\,(x/s-2.25\,|y/s|-0.85)$ and wing bending represented by $f_{2w}=(y/s)\,|y/s|$. The horizontal tail modes are: tail roll represented by $f_{1t}=y/s$ and tail pitch represented by $f_{2t}=[\,(x-x_{ta})/s]\,(y/|y|)$ (the values of x_{ta} are $x_{ta}=3.35, 3.75$, and 4.2 for $z_0/s=0, 0.6$, and 1.2, respectively). The results relating to the above configuration using the four antisymmetric modes at two reduced frequencies ($k=\omega s/v$) $k_1\approx 0$ and $k_2=1.5$ are presented in Table 3. At this stage, mention should be made that in evaluating the unsteady acceleration potential kernel function, as represented by Eq. (2), two incomplete Struve functions need to be computed. These two incomplete Struve functions can be evaluated in approximate terms only. The accuracy of two approximate algorithms is tested in Ref. 17 against the accuracy of the commonly used approximation due to Laschka.[18] The present version of the PCKFM incorporates the D 12.1 approximation of Ref. 17 (see Appendix herein for more details) to evaluate the unsteady kernel function. As shown in Ref. 17, the D 12.1 approximation reduces the error in evaluating the modified Struve function by two orders of magnitude, as compared with the commonly used Laschka approximation, at the ex-

Table 3[a] Comparison study of antisymmetric nonplanar wing-tail configuration computed by different methods, $M=0.8$ $z/s=0.6$

Generalized force in	Caused by pressure in	i,j	$k\approx 0.0$ Q/deg		$k=1.5$ Q/deg		Method of computation
Wing twist	Wing twist	1,1	0.1645	110.6	0.2231	130.5	Present
			0.1822	114.5	0.2563	132.4	Ref. 13
			0.1933	116.8	0.2820	136.2	Ref. 15
			0.1791	114.0	0.2420	132.6	Ref. 8
			0.1832	115.1	0.2527	135.0	Ref. 16
Wing bending	Wing twist	2,1	0.4411	52.4	0.4416	58.0	Present
			0.4509	54.7	0.4522	60.8	Ref. 13
			0.4614	55.5	0.4668	62.6	Ref. 15
			0.4696	53.7	0.4564	60.5	Ref. 8
			0.4537	55.0	0.4418	63.0	Ref. 16
Wing bending	Wing bending	2,2	0.1859	90.0	0.3815	146.8	Present
			0.1843	90.0	0.3898	147.4	Ref. 13
			0.1842	90.0	0.4054	149.1	Ref. 15
			0.1964	90.0	0.3936	146.9	Ref. 8
			0.1837	90.0	0.3829	147.9	Ref. 16
Tail pitch	Tail roll	4,3	0.1575	90.0	0.3374	146.0	Present
			0.1587	90.0	0.3612	148.0	Ref. 13
			0.1519	90.0	0.3610	149.6	Ref. 15
			0.1725	90.0	0.3503	144.8	Ref. 8
			0.1577	90.0	0.3561	147.4	Ref. 16
Tail pitch	Tail pitch	4,4	0.5772	71.6	0.6621	92.2	Present
			0.6238	73.2	0.6846	95.1	Ref. 13
			0.5913	71.6	0.6458	94.0	Ref. 15
			0.6218	71.1	0.6539	91.2	Ref. 8
			0.6067	72.1	0.6344	91.5	Ref. 16

[a]All the results, except the present one, are reproduced from Ref. 4.

Table 4 Comparison study of antisymmetric nonplanar wing-tail configuration (dihedral and anhedral tails for $k \approx 0.0$, $M = 0.8$, $z/s = 0.6$)

Generalized force in	Caused by pressure in	i,j	Dihedral 30 deg, Q	/deg	Dihedral 0 deg, Q	/deg	Anhedral 30 deg, Q	/deg	Method of computation
Wing twist	Wing twist	1,1	0.1613	110.6	0.1645	110.6	0.1619	110.6	Present
			0.1933	116.8	0.1933	116.8	0.1943	116.9	Ref. 15
Wing bending	Wing twist	2,1	0.4409	52.3	0.4411	52.4	0.4416	52.5	Present
			0.4613	55.5	0.4514	55.5	0.4617	55.8	Ref. 15
Wing bending	Wing bending	2,2	0.1861	90.0	0.1859	90.0	0.1857	90.0	Present
			0.1843	90.0	0.1842	90.0	0.1832	90.0	Ref. 15
Tail pitch	Tail roll	4,3	0.1516	90.0	0.1575	90.0	0.1510	90.0	Present
			0.1484	90.0	0.1519	90.0	0.1478	90.0	Ref. 15
Tail pitch	Tail pitch	4,4	0.5405	71.0	0.5772	71.6	0.5432	71.3	Present
			0.5759	71.7	0.5913	71.6	0.5782	72.0	Ref. 15

Table 5 Comparison study of antisymmetric nonplanar wing-tail configuration (dihedral and anhedral tails for $k = 1.5$, $M = 0.8$, $z/s = 0.6$)

Generalized force in	Caused by pressure in	i,j	Dihedral 30 deg, Q	/deg	Dihedral 0 deg, Q	/deg	Anhedral 30 deg, Q	/deg	Method of computation
Wing twist	Wing twist	1,1	0.2231	130.5	0.2231	130.5	0.2230	130.6	Present
			0.2819	136.2	0.2820	136.8	0.2820	136.0	Ref. 15
Wing bending	Wing twist	2,1	0.4416	58.0	0.4416	58.0	0.4413	58.0	Present
			0.4667	62.7	0.4668	62.6	0.4680	62.5	Ref. 15
Wing bending	Wing bending	2,2	0.3815	146.8	0.3815	146.8	0.3805	147.0	Present
			0.4054	149.1	0.4054	149.1	0.4059	149.0	Ref. 15
Tail pitch	Tail roll	4,3	0.3161	144.2	0.3374	146.0	0.3154	144.1	Present
			0.3455	149.7	0.3610	149.6	0.3455	149.5	Ref. 15
Tail pitch	Tail pitch	4,4	0.5848	88.8	0.6221	92.2	0.5839	91.3	Present
			0.5176	94.7	0.6458	94.0	0.6173	93.7	Ref. 15

pense of a negligible increase in computation time. The generalized aerodynamic forces are defined following Ref. 8. The PCKFM is coded to run on the IBM 3081D computer installed at the Technion—Israel Institute of Technology using the IBM double-precision mode.

Table 3 shows a comparison study of some of the aerodynamic coefficients as computed by several methods.[13,15,8,16] It can be seen that the present results compare well with those obtained using the alternate methods. It seems that the PCKFM results correlate best with those of Akamatsu.[13] The method of Ref. 13 is based on a kernel function method type, while the other methods are based on the doublet-lattice method. The results of the present method are believed to be more accurate due to the special attention paid while performing spanwise integration of Eq. (2) (i.e., without artificially increasing its singularity) and due to a more accurate algorithm for computing the modified Struve function that affects the accuracy of the unsteady kernel function. Tables 4 and 5 represent similar results for the same AGARD configuration, but with an elevated fold tail (instead of the unfolded elevated $z/s = 0.6$ tail used in Table 3). The horizontal tail is folded with a dihedral or anhedral of 30 deg. Table 4 represents the results assuming a reduced frequency of $k = 0.01$, while Table 5 represents similar results using a reduced frequency of $k = 1.5$. Tables 4 and 5 compare results obtained using the PCKFM and the method of Ref. 15. Even though the results yielded by the two methods differ appreciably from each other, the trend of the changes due to the folded tail is the same. It can be seen that the anhedral effect is more dominant than the dihedral effect since the anhedral brings the tail closer to the wing surface plane and, thus, closer to the wing vortices' shedding plane. It appears that the PCKFM results show the anhedral effects more sharply than those obtained using the method of Ref. 15.

Conclusions

The piecewise continuous kernel function method (PCKFM) is tested herein for a nonplanar configuration both in a steady flow and in antisymmetric vibration modes. The results obtained are compared with those obtained using other methods. This comparison confirms the ability of the method to compute unsteady aerodynamic forces of nonplanar configurations at subsonic flows. It is shown that the nonplanar part of the kernel function has the same order of singularity as the planar part, and that there is no need to increase artificially the order of the kernel singularity from a second to a fourth-order pole. In most of the cases considered, the difference between the values of the aerodynamic coefficients, as obtained by the various other methods (including the lattice methods), and those obtained by the present method, are within reasonable limits. This is due to the differences in the computation algorithms, including differences in computation of the kernel function. It is shown that the PCKFM yields converged results with a very small number of pressure polynomials and a minimum number of boxes (i.e., two boxes). The rapid convergence characteristics of the PCKFM are once again demonstrated together with its inherent efficiency and reduced computational labor.

Appendix

The incomplete modified Struve function for computing K_1 and K_2 of the unsteady kernel function of Eq. (3) can be rescaled to (see Ref. 17)

$$F(s,r) = \int_s^\infty e^{-irt}(1+t^2)^{-3/2}\mathrm{d}t \tag{A1}$$

and

$$G(s,r) = \int_s^\infty e^{-irt}(1+t^2)^{-5/2}\mathrm{d}t \tag{A2}$$

In subsonic flow the upper limit of integration is infinity, as in Eqs. (A1) and (A2). In supersonic flow, the upper limit is variable so that the integrals are expressed as differences of the incomplete Struve function of the types indicated by Eqs. (A1) and (A2). The integrals represented by Eqs. (A1) and (A2) can be brought to the following form using integration by parts:

$$F(s,r) = \int_s^{\infty} e^{-irt}\left(1 - \frac{t}{\sqrt{1+t^2}}\right)\mathrm{d}t \tag{A3}$$

and

$$G(s,r) = \int_s^{\infty} e^{-irt}t\left(1 - \frac{t}{\sqrt{1+t^2}}\right)\mathrm{d}t \tag{A4}$$

The function to be approximated by exponential expansion is

$$f(t) = 1 - \frac{t}{\sqrt{1+t^2}} \tag{A5}$$

The commonly used approximation to $f(t)$ is the 11-term exponential polynomial

$$f(t) \sim g(t) = \sum_{k=1}^{11} a_k \exp(-kbt) \tag{A6}$$

and is due to Laschka.[9] The exponent b and coefficient a_k appearing in Eq. (A6) are tabulated in previous papers.[17] Equation (A6) can be used only if t is non-negative. If t is negative, then $g(t) = 2 - g(|t|)$.

The purpose of the study conducted in Ref. 17 was to obtain a better approximation to $f(t)$ while maintaining the computational efficiency of Laschka's[9] approximation. It was suggested[17] that $f(t)$ be expanded using

$$g(t) = \sum_{k=1}^{n} a_k \exp(2^{k/m}bt) \tag{A7}$$

The series that replaces the Laschka approximation and is represented by Eq. (A7) is designated as D 12.1 and is defined as follows:

$$n = 12, \quad m = 1, \quad b = 0.009054814793$$

$a_1 =$	0.000319759140	$a_2 =$	−0.000055461471
$a_3 =$	0.002726074362	$a_4 =$	0.005749551566
$a_5 =$	0.031455895072	$a_6 =$	0.106031126212
$a_7 =$	0.406838011567	$a_8 =$	0.798112357155
$a_9 =$	−0.417749229098	$a_{10} =$	0.077480713894
$a_{11} =$	−0.012677284771	$a_{12} =$	0.001787032960

Approximation D 12.1 can be used to evaluate rapidly the integrals represented by Eqs. (A1) and (A2). As stated earlier, the use of the D 12.1 series, instead of Laschka's approximation, reduces the maximum error $|f(t) - g(t)|$ by two orders of magnitude as compared to Laschka's approximation at the expense of a negligible increase in execution time.[17]

References

[1]Landahl, M. T. and Stark, V.J.E., "Numerical Lifting Surface Theory—Problems and Progress," *AIAA Journal,* Vol. 6, Nov. 1968, pp. 2049-2060.

[2]Laschka, B., "Interfering Lifting Surfaces in Subsonic Flow," *Zeitschrift fuer Flugwissenschaften,* Band 18, Heft 9/10, 1970.

[3]Ashley, H. and Rodden, W. P., "Wing-Body Aerodynamic Interaction," *Annual Review of Fluid Mechanics,* Vol. 4, 1972, pp. 431-472.

[4]Rodden, W. P., "A Comparison of Methods Used in Interfering Lifting Surface Theory," *Supplement to the Manual on Aeroelasticity,* Vol. VI, AGARD-R-643.

[5]Lottati, I. and Nissim, E., "Three-Dimensional Oscillatory Piecewise Continuous Kernel Function Method—Part I: Basic Problems," *Journal of Aircraft,* Vol. 18, May 1981, pp. 346-351.

[6]Lottati, I. and Nissim, E., "Three-Dimensional Oscillatory Piecewise Continuous Kernel Function Method—Part II: Geometrically Continuous Wings," *Journal of Aircraft,* Vol. 18, May 1981, pp. 352-355.

[7]Lottati, I. and Nissim, E., "Three-Dimensional Oscillatory Piecewise Continuous Kernel Function Method—Part III: Wings with Geometrical Discontinuities," *Journal of Aircraft,* Vol. 18, May 1981, pp. 356-363.

[8]Rodden, W. P., Giesing, J. P, and Kalman, T. P., "New Developments and Applications of the Subsonic Doublet-Lattice Method for Nonplanar Configurations," *AGARD Symposium on Unsteady Aerodynamics for Aeroelastic Analyses of Interfering Surfaces,* Tonsberg, Norway, AGARD-CP-80-71, April 1971, pp. 4.1-4.27

[9]Laschka, B., "Das Potential und des Geschwindigkeitsfeld der harmonish schwingenden tragenden Flache bei Unterschallstromung," *Zeitschrift fur Angewandte Mathematik und Mechanik,* Vol. 43, 1963b, pp. 325-333, and Vol. 47, 1967, p. 284.

[10]Vivian, H. T. and Andrew, L. V., "Unsteady Aerodynamics for Advanced Configurations. Part I—Application of the Subsonic Kernel Function to Nonplanar Lifting Surfaces," AFFDL-TDR-64-152, 1965.

[11]Landahl, M. T., "Kernel Function for Nonplanar Oscillating Surfaces in a Subsonic Flow," *AIAA Journal,* Vol. 5, May 1967, pp. 1045-1046.

[12]Rodden, W. P., Giesing, J. P., and Kalman, T. P., "Refinement of the Nonplanar Aspects of the Subsonic Doublet-Lattice Lifting Surface Method," *Journal of Aircraft,* Vol. 9, Jan. 1972, pp. 69-73.

[13]Akamatsu, Y., "ONERA's Calculations on Interfering Lifting Surfaces," ONERA Paper, 1974; contribution to AGARD-R-643.

[14]Mykytow, W. J., Olsen, J. J., and Pollock, S. J., "Application of AFFDL Unsteady Load Prediction Methods to Interfering Surfaces," *AGARD Symposium on Unsteady Aerodynamics for Aeroelastic Analyses of Interfering Surfaces,* Tonsberg, Norway, AGARD-CP-80-71, April 1971, pp. 7.1-7.21.

[15]Huttsell, L. J. and Pollock, S. J., "Unsteady Aerodynamic Loads for the AGARD Interfering Lifting Surfaces," AFFDL Paper, 1974; contribution to AGARD-R-643.

[16]Schmid, H. and Becker, J., "Contribution to the AGARD Programme on Unsteady Aerodynamics for Interfering Surfaces," MBB Paper, 1973; contribution to AGARD-R-643.

[17]Desmarais, R. N., "An Accurate and Efficient Method for Evaluating the Kernel of the Integral Equation Relating Pressure to Normal Wash in Unsteady Potential Flow," AIAA Paper 82-0687, 1982.

[18]Laschka, B., "Interfering Lifting Surfaces in Subsonic Flow," paper presented at the 29th AGARD Structures and Materials Panel Meeting, Istanbul, Turkey, 1969.